

## The crystal structure of a high-pressure polymorph of $\text{CaSiO}_3$

By FELIX J. TROJER

Crystallographic Laboratory, Massachusetts Institute of Technology  
Cambridge, Massachusetts

(Received 16 December 1968)

### Auszug

Diese Hochdruckphase des  $\text{CaSiO}_3$  kristallisiert in der Raumgruppe  $P\bar{1}$  und hat folgende Zelldimensionen:  $a = 6,695 \text{ \AA}$ ,  $b = 9,257 \text{ \AA}$ ,  $c = 6,666 \text{ \AA}$ ,  $\alpha = 86^\circ 30'$ ,  $\beta = 76^\circ 08'$  und  $\gamma = 70^\circ 23'$ . Die Struktur wurde mit Hilfe der Patterson-Methode gelöst. Die dabei gewonnenen vorläufigen Atomkoordinaten sind nach der Methode der kleinsten Quadrate bis zu einem  $R$ -Wert von 6,5% verfeinert worden. Die Hauptmerkmale dieser Struktur sind: irreguläre Ca-Lagen, die jeweils durch zwei Ca-Atome verbunden sind; in den Hohlräumen zwischen den Schichten befinden sich  $\text{Si}_3\text{O}_9$ -Ringe.

### Abstract

This high-pressure phase of  $\text{CaSiO}_3$  crystallizes in space group  $P\bar{1}$  with following cell dimensions:  $a = 6.695 \text{ \AA}$ ,  $b = 9.257 \text{ \AA}$ ,  $c = 6.666 \text{ \AA}$ ,  $\alpha = 86^\circ 30'$ ,  $\beta = 76^\circ 08'$  and  $\gamma = 70^\circ 23'$ . The structure was solved by interpretation of the Patterson function. Preliminary coordinates obtained in this procedure were refined by least-squares methods until the  $R$  value dropped to 6.5%. The basic features of this structure are irregular layers of Ca atoms which are interconnected by pairs of Ca atoms and  $\text{Si}_3\text{O}_9$  rings which are located in the remaining space in between the layers.

### Introduction

The first structure proposal with  $\text{Si}_3\text{O}_9$  rings as a feature of a phase of calcium metasilicate was made by BARNIK (1936) for the monoclinic variety of wollastonite, a proposal which was criticized by many crystal-structure analysts. Meanwhile other modifications of  $\text{CaSiO}_3$  or chemically similar compounds were studied, in none of which rings have been definitely revealed.

In this context JEFFERY and HELLER (1953) made a preliminary x-ray investigation for a high-temperature phase of  $\text{CaSiO}_3$  known as

pseudowollastonite. With oscillation, rotation, and Weissenberg photographs these authors were able to determine the symmetry to be pseudo-hexagonal which might well allow for  $\text{Si}_3\text{O}_9$  rings. Unfortunately the crystals were not good enough to proceed with a detailed structure determination. In the meantime BARNIK's ring proposal for monoclinic wollastonite was proven incorrect by MAMEDOV and BELOV (1956). The Russian authors found  $\text{SiO}_3$  chains to be the basic structural feature in wollastonite. Considering the limited results given by JEFFERY and HELLER for pseudowollastonite, HILMER (1963) tried to avoid the difficulty encountered with bad crystalline material by solving a structurally analogous compound. LIEBAU (1960) had suggested that  $\text{SrGeO}_3$ ,  $\text{SrSiO}_3$ , and the low-temperature phase of  $\text{BaGeO}_3$  were structural analogs of pseudowollastonite. HILMER selected  $\text{SrGeO}_3$  and succeeded in determining the structure in which she found  $\text{Ge}_3\text{O}_9$  rings. On the basis of this investigation HILMER suggested that the results obtained with  $\text{SrGeO}_3$  also apply to the structure of pseudowollastonite. Encouraged by these findings, the present project was undertaken to examine a high-pressure, high-temperature polymorph of calcium metasilicate with the hope of answering the following two questions: first, what is the arrangement of the silicon-oxygen tetrahedra and, second, is there any relation to the structure proposed by HILMER for pseudowollastonite.

### Material

The specimen for this investigation was synthesized by Dr. R. D. SHANNON of the Central Research Department, E. I. du Pont de Nemours and Co., and was kindly made available by Dr. CHARLES T. PREWITT. The crystals were made from  $\text{CaSiO}_3$  glass at 65 kilobars and approximately  $1300^\circ\text{C}$ . A density of  $3.05\text{ g/cm}^3$  was determined by the immersion method using a mixture of methylene iodide ( $\rho = 3.32\text{ g/cm}^3$ ) and methyl iodide ( $\rho = 2.28\text{ g/cm}^3$ ). This density is considerably higher than the value of  $2.88\text{ g/cm}^3$  found for wollastonite.

The pressure and temperature conditions mentioned above are within the stability field for another new phase of  $\text{CaSiO}_3$  observed by RINGWOOD and MAJOR (1967). These two Australian scientists report that wollastonite is stable up to 30 kilobars. Above this pressure they observed a new phase which is characterized by a density higher than that of wollastonite and by a powder pattern very similar to the one made from this sample. They found their phase to be stable

up to pressures well above 100 kilobars. The strong similarities in stability field, powder pattern, and density suggest a close structural resemblance, if not actually identity, of these two phases.

### Space group and cell dimensions

Precession photographs showed triclinic symmetry, indicating one of the two space groups  $P1$  and  $P\bar{1}$ . The choice of  $P\bar{1}$  as the correct space group was based on a statistical analysis of the  $|F_{\text{obs}}|$ . According to KARLE and HAUPTMAN (1958), centrosymmetric structures have theoretical statistical averages of their normalized structure factors,  $|E|$ , as listed in Table 1. This table also shows the close resemblance of the observed values for the CaSiO<sub>3</sub> phase examined in this investigation and the theoretical values for a centrosymmetric structure.

Table 1. *Theoretical and observed statistical averages of normalized structure factors*

Nature of average	Expected for centrosymmetric structures	Observed
$\langle  E  \rangle$	0.798	0.785
$\langle  E^2 - 1  \rangle$	0.968	0.992
$\langle E^2 - 1 \rangle$	0.0	0.0

A set of back-reflection Weissenberg photographs was used to determine precise lattice constants. These film data were refined by the least-squares method. The cell dimensions are given in Table 2.

Table 2. *Symmetry and cell data for the high-pressure polymorph of CaSiO<sub>3</sub>*

Space group:	$P\bar{1}$	
Cell dimensions:	$a = 6.695 \pm 0.005 \text{ \AA}$	$\alpha = 86^\circ 38' \pm 3'$
	$b = 9.257 \pm 0.007 \text{ \AA}$	$\beta = 76^\circ 08' \pm 3'$
	$c = 6.666 \pm 0.006 \text{ \AA}$	$\gamma = 70^\circ 23' \pm 2'$
Density observed:	3.05 g/cm <sup>3</sup>	
Density calculated:	3.06 g/cm <sup>3</sup> for $Z = 6$	
Density of wollastonite:	2.88 g/cm <sup>3</sup>	

### Measurement of the intensities

Most of the crystals of the new high-pressure phase were either too small or of too poor quality to be used for intensity measurement. Finally, after examining about 40 specimens, a suitable crystal with

Table 3. Observed and computed structure factors (in electron units)

h k l	$ F_o $	$F_c$	h k l	$ F_o $	$F_c$	h k l	$ F_o $	$F_c$	h k l	$ F_o $	$F_c$	h k l	$ F_o $	$F_c$		
0 0 1	10.2	10.3	-5 1 0	18.1	15.1	2 1 5	33.5	32.9	-2 2 2	74.9	76.7	6 2 0	14.9	17.0		
2 4 4	31.6		1 20.5	23.2	6 6	13.9	14.1	3 41.4	43.7	1 41.2	44.1	1 41.2	44.1			
3 10.1	8.1		2 36.4	39.8	7 4.7	5.3	4 28.9	-24.0	2 50.9	52.3	2 50.9	52.3				
4 3.0	-1.8		3 6.9	6.8	3 1 -6	26.3	-25.7	5 9.9	11.2	3 28.2	29.8	3 28.2	29.8			
5 22.4	19.4		4 8.9	8.3	-5 13.5	-13.8	6 0.0	-1.4	4 11.6	-12.2	4 11.6	-12.2				
6 74.3	-70.9		-4 1 -7	7.9	11.8	-4 3.1	3.1	-1 2 -7	14.8	-16.6	5 27.0	30.0	5 27.0	30.0		
7 22.2	61.8		-6 20.3	-18.6	-3 23.4	-20.5	-6 8.6	-9.4	-5 5.1	-9.2	3 11.3	-12.8	3 11.3	-12.8		
1 0 -6	5.1	4.3	-5 19.9	19.3	-2 22.1	-21.2	-5 8.6	8.5	7 2 -1	9.9	-13.1	0 4.2	-4.8	0 4.2	-4.8	
-5 4.8	-4.8		-4 2.0	2.3	-1 37.4	-36.4	-3 25.5	27.8	-2 18.6	-18.0	1 30.6	-31.1	1 30.6	-31.1		
-4 55.4	-55.5		-3 5.5	-2.0	0 74.7	69.3	0 74.7	69.3	-1 42.7	38.5	2 22.9	24.6	2 22.9	24.6		
-3 25.8	-25.3		-2 38.4	-36.9	1 51.8	47.9	0 14.6	5.5	1 47.3	-47.8	4 16.0	17.6	4 16.0	17.6		
-2 31.2	-29.5		-1 27.1	-25.5	2 40.2	37.2	1 47.3	-47.8	2 43.4	44.6	-5 3 -5	15.5	14.1	-5 3 -5	15.5	14.1
-1 1.4	-1.8		0 20.9	19.7	3 14.8	-14.5	3 0.0	-2.0	3 0.0	-2.0	-3 47.9	50.1	-3 47.9	50.1		
0 2.6	-0.1		1 41.9	-40.8	4 25.9	-26.4	4 15.9	19.1	-2 13.8	16.0	0 0.0	0.8	0 0.0	0.8		
1 17.7	-17.1		2 22.1	-20.9	5 2.5	-1.8	5 2.5	-1.8	-4 5	5.0	-4 5	5.0	-4 5	5.0		
2 68.2	64.8		3 2.0	-0.3	6 32.3	-33.3	6 32.3	-33.3	4 31.3	29.0	-1 4.2	6.7	-1 4.2	6.7		
3 65.2	60.1		4 23.6	23.0	7 3.3	-2.7	7 3.3	-2.7	7 33.6	32.7	2 0.0	0.7	2 0.0	0.7		
4 40.7	39.7		5 9.3	8.5	4 1 -5	31.7	29.9	0 2 -7	1.1	2.5	-4 5 -6	11.6	-11.9	-4 5 -6	11.6	-11.9
5 16.9	16.0		-3 1 -7	11.6	-10.8	-4 26.2	23.8	-6 20.4	-20.6	-5 24.3	24.3	-5 24.3	24.3	-5 24.3	24.3	
6 18.6	-16.1		-6 52.6	53.3	-5 7.7	-7.3	-5 7.7	-7.3	-4 30.5	30.7	-3 13.5	13.4	-3 13.5	13.4		
7 28.3	26.9		-5 54.7	51.8	-2 22.0	-18.9	-2 22.0	-18.9	-2 52.3	-52.2	-1 48.1	50.8	-1 48.1	50.8		
-6 30.6	30.2		-4 9.7	-9.1	-1 9.9	-8.4	-1 9.9	-8.4	1 15.8	-16.8	2 24.3	24.3	2 24.3	24.3		
-5 39.2	37.8		-2 32.9	-30.9	1 15.6	-15.3	1 15.6	-15.3	-3 40.0	41.5	-2 13.5	13.4	-2 13.5	13.4		
-4 24.0	-23.0		-1 25.6	23.0	2 29.0	-28.2	2 29.0	-28.2	-2 52.3	-52.2	-2 28.7	-32.9	-2 28.7	-32.9		
-3 9.1	-9.3		0 13.0	-10.8	3 46.0	44.5	3 46.0	44.5	1 28.0	-29.8	-1 48.1	50.8	-1 48.1	50.8		
-2 11.9	11.6		1 32.7	-30.7	4 43.0	-42.8	4 43.0	-42.8	4 31.3	29.0	0 43.7	43.7	0 43.7	43.7		
-1 60.0	-56.9		2 19.5	20.5	5 10.4	-10.5	5 10.4	-10.5	4 45.9	45.4	-3 3 -7	2.7	2.2	-3 3 -7	2.7	2.2
0 109.9	-99.4		3 44.4	-44.6	6 17.0	-16.6	6 17.0	-16.6	5 29.3	-27.7	-6 11.8	10.9	-6 11.8	10.9		
1 56.2	-48.8		4 16.2	16.4	7 12.0	-11.3	7 12.0	-11.3	6 8.4	8.2	-5 27.4	-26.1	-5 27.4	-26.1		
2 21.7	18.9		5 6.4	-7.4	8 0.0	-1.1	8 0.0	-1.1	7 4.0	2.5	-4 18.5	-19.0	-4 18.5	-19.0		
3 26.5	-25.1		6 32.3	-28.8	3 29.6	27.6	3 29.6	27.6	1 2 -7	15.8	-16.8	-3 60.2	-62.3	-3 60.2	-62.3	
4 32.7	-31.1		-2 1 -7	21.4	-21.7	-2 9.3	-9.8	-2 9.3	-9.8	-5 19.7	20.9	-1 14.4	-15.6	-1 14.4	-15.6	
5 17.4	-16.6		-6 26.6	26.8	0 9.1	-9.1	0 9.1	-9.1	-4 5.5	-5.3	0 7.0	-10.2	0 7.0	-10.2		
6 45.0	42.8		-4 18.9	-18.3	1 41.6	-40.3	1 41.6	-40.3	1 5.8	10.5	1 34.6	36.5	1 34.6	36.5		
7 17.4	5.1		-3 28.0	28.8	2 8.1	8.8	2 8.1	8.8	-2 47.2	46.4	2 24.3	24.3	2 24.3	24.3		
3 0 -6	22.2	20.9	-2 68.1	65.6	3 6.9	-7.5	3 6.9	-7.5	-1 14.0	14.2	3 43.5	42.9	3 43.5	42.9		
-5 18.2	17.3		-1 40.7	35.7	4 39.8	39.1	4 39.8	39.1	1 13.9	-13.3	4 12.5	14.6	4 12.5	14.6		
-4 12.8	9.9		0 43.9	-39.7	5 5.4	3.9	5 5.4	3.9	2 44.9	-44.1	5 0.7	0.8	5 0.7	0.8		
-3 62.9	62.4		-1 5.4	5.5	6 6.4	-6.3	6 6.4	-6.3	3 12.6	-13.1	-2 5	4.9	-2 5	4.9		
-2 0.6	-0.6		2 47.5	47.5	7 28.0	29.4	7 28.0	29.4	4 31.1	-31.6	-2 24.3	-22.3	-2 24.3	-22.3		
-1 27.0	25.4		3 17.9	-17.9	6 1 -3	12.7	11.9	6 1 -3	12.7	11.9	-4 20.2	-19.9	-4 20.2	-19.9		
0 20.4	-18.3		4 10.7	-11.2	-2 11.4	9.1	-2 11.4	9.1	6 46.8	-45.1	-3 9.4	-8.5	-3 9.4	-8.5		
1 5.8	5.6		5 29.6	-28.2	-1 26.4	26.2	-1 26.4	26.2	7 18.9	-16.8	-2 5.9	3.5	-2 5.9	3.5		
2 4.4	-1.2		6 23.8	-26.3	0 67.3	-64.8	0 67.3	-64.8	2 2 -7	24.6	-25.0	-1 50.3	-50.9	-1 50.3	-50.9	
3 71.2	-67.9		7 14.8	-14.9	1 21.4	20.4	1 21.4	20.4	-5 48.3	-50.0	0 63.6	-62.4	0 63.6	-62.4		
4 50.0	-49.5		-6 52.4	-52.3	2 14.9	15.5	2 14.9	15.5	-4 25.0	-25.5	1 21.2	-22.2	1 21.2	-22.2		
5 18.2	-17.0		-5 51.4	-49.9	3 50.8	-50.5	3 50.8	-50.5	-3 5.4	6.2	2 5.4	3.5	2 5.4	3.5		
6 4.8	5.6		-4 2.6	0.0	4 16.6	-16.7	4 16.6	-16.7	-2 29.5	30.5	3 4.6	3.9	3 4.6	3.9		
4 0 -5	23.1	-20.9	-3 42.2	41.0	5 29.6	-31.9	5 29.6	-31.9	1 52.6	-52.9	-1 36.9	-39.7	-1 36.9	-39.7		
-3 10.2	8.1		-2 6.9	-7.0	6 37.8	37.7	6 37.8	37.7	0 46.2	-42.1	5 10.1	11.0	5 10.1	11.0		
-2 43.5	-40.8		-1 27.9	-25.2	7 1 -1	0.0	-3.4	7 1 -1	0.0	-3.4	1 102.7	94.8	1 102.7	94.8		
-1 41.4	37.3		0 4.4	-4.0	0 3.7	-0.1	0 3.7	-0.1	2 9.4	8.3	-1 3	6.7	-1 3	6.7		
0 26.7	22.8		1 11.6	10.9	1 7.1	8.9	1 7.1	8.9	3 12.7	-12.6	-6 1.5	-0.6	-6 1.5	-0.6		
1 36.6	35.1		2 66.4	-65.5	2 7.7	-7.7	2 7.7	-7.7	2 2 -7	-1.8	-5 2.2	4.0	-5 2.2	4.0		
2 26.6	-24.3		3 27.4	26.2	3 7.6	-12.0	3 7.6	-12.0	5 0.0	-2.2	-5 51.3	51.3	-5 51.3	51.3		
3 18.3	15.8		4 21.9	-20.6	4 3.8	-4.9	4 3.8	-4.9	6 35.3	34.8	-3 1.4	0.8	-3 1.4	0.8		
4 88.1	84.3		5 24.7	23.8	-6 2 -4	14.3	-14.3	-6 2 -4	14.3	-14.3	-2 78.9	78.1	-2 78.9	78.1		
5 36.9	-35.3		6 24.1	21.9	-3 13.6	-15.1	-3 13.6	-15.1	7 24.2	-23.9	-1 40.5	-38.7	-1 40.5	-38.7		
6 18.2	-17.9		7 29.2	-28.5	-5 2 -6	5.1	-5.1	-5 2 -6	5.1	-5.1	0 2.5	-3.0	0 2.5	-3.0		
7 24.0	-22.7		0 1 -7	11.6	11.8	-5 10.8	11.5	-5 10.8	11.5	-4 26.5	26.3	1 20.9	22.5	1 20.9	22.5	
5 0 -4	18.7	-17.4	-6 10.1	11.7	-4 22.0	21.6	-4 22.0	21.6	-3 85.6	-82.9	2 10.5	-12.4	2 10.5	-12.4		
-3 49.5	-46.4		-5 10.5	-8.4	-3 18.5	-18.9	-3 18.5	-18.9	-2 20.9	-19.4	3 17.8	-18.5	3 17.8	-18.5		
-2 5.5	6.6		-4 29.5	29.8	-2 0.1	-1.5	-2 0.1	-1.5	-1 46.2	-43.7	4 57.1	-59.7	4 57.1	-59.7		
-1 30.8	-29.0		-3 67.2	-67.8	-1 15.9	-15.1	-1 15.9	-15.1	0 56.5	-51.4	5 4.3	-2.2	5 4.3	-2.2		
0 11.7	-11.6		-2 85.3	-84.9	0 18.6	-20.0	0 18.6	-20.0	1 53.3	49.3	6 2.9	6.0	6 2.9	6.0		
1 13.7	12.3		-1 4.6	-2.6	2 2.3	-3.0	2 2.3	-3.0	2 15.6	-14.5	0 3	-7.4	0 3	-7.4		
2 33.2	-31.2		1 10.0	-8.1	-4 2 -6	28.2	-27.0	-4 2 -6	28.2	-27.0	-6 73.8	-75.4	-6 73.8	-75.4		
3 54.6	52.6		2 53.5	-54.0	-5 0.0	0.0	-5 0.0	0.0	4 4.2	4.3	-5 2.7	2.7	-5 2.7	2.7		
4 10.8	10.2		3 20.3	21.5	-4 6.2	5.8	-4 6.2	5.8	5 6.1	4.6	-4 9.7	10.6	-4 9.7	10.6		
5 15.4	13.6		4 23.6	23.4	-3 5.5	6.4	-3 5.5	6.4	6 63.2	62.7	-3 16.8	-18.3	-3 16.8	-18.3		
6 0 -3	10.2	-10.3	5 20.5	-20.3	-2 16.4	-16.6	-2 16.4	-16.6	7 1.1	-3.2	-2 18.0	18.6	-2 18.0	18.6		
-2 13.5	16.1		-6 6.2	-7.0	-1 42.7	-43.5	-1 42.7	-43.5	4 2 -5	19.7	20.1	0 140.3	139.9	0 140.3	139.9	
-1 6.4	-6.0		7 1.4	1.4	0 32.6	-33.7	0 32.6	-33.7	-4 29.5	30.4	1 36.9	35.8	1 36.9	35.8		
0 32.5	-37.5		1 1 -7	17.3	17.2	1 21.7	-22.6	1 21.7	-22.6	-3 14.1	-12.8	2 38.8	-38.2	2 38.8	-38.2	
1 9.0	-9.6		-6 25.2	24.6	2 25.2	-24.5	2 25.2	-24.5	-2 42.1	-43.1	3 64.5	66.6	3 64.5	66.6		
2 4.8	-7.1		-5 10.9	9.0	3 14.1	-13.6	3 14.1	-13.6	-1 24.7	-24.4	4 19.5	18.9	4 19.5	18.9		
3 7.8	5.9		-4 30.2	29.8	4 6.4	-6.5	4 6.4	-6.5	0 6.3	5.2	5 22.8	23.0	5 22.8	23.0		
4 25.2	-20.2		-3 43.8	-43.3	-3 2 -7	4.0	-3.7	-3 2 -7	4.0	-3.7	6 32.1	-32.2	6 32.1	-32.2		
5 10.7	14.0		-2 56.7	54.5	-6 3.1	-3.5	-6 3.1	-3.5	2 66.0	-65.6	7 14.2	-12.4	7 14.2	-12.4		
7 0 -1	1.8	1.6	-1 7.6	-7.3	-5 3.2	-3.7	-5 3.2	-3.7	3 0.9	3.3	1 3	-7.4	1 3	-7.4		
0 2.7	-6.5		1 47.0	41.6	-4 0.0	-3.3	-4 0.0	-3.3	4 8.3	-9.2	-6 9.8	-10.7</				

Table 3. (Continued)

h k l	F <sub>o</sub>	F <sub>c</sub>	h k l	F <sub>o</sub>	F <sub>c</sub>	h k l	F <sub>o</sub>	F <sub>c</sub>	h k l	F <sub>o</sub>	F <sub>c</sub>	h k l	F <sub>o</sub>	F <sub>c</sub>
2 3 -1	39.4	42.6	-1 4 -4	16.6	16.8	7 4 -1	8.8	7.4	3 5 3	4.3	-2.7	1 6 3	2.5	0.5
0	64.9	-69.5	-3	25.1	-25.2	0	11.5	-13.4	4	19.6	18.4	4	31.1	29.8
1	16.3	-14.8	-2	6.8	-7.0	1	18.6	19.3	5	4.9	3.0	5	18.7	16.7
2	6.6	-7.5	-1	20.4	-20.3	2	3.2	2.0	6	53.8	54.8	6	26.7	-25.6
3	44.6	-47.4	0	13.2	-14.6	3	3.4	1.7	7	7.8	-7.8	2 6 -6	31.4	32.2
5	23.8	-25.6	1	48.2	48.3	4	12.7	-12.9	-5	15.9	18.1	-5	7.5	9.3
6	39.2	40.9	2	15.1	-15.7	5	15.1	-11.7	-4	38.0	39.3	-4	14.2	-16.6
7	15.7	16.1	3	5.8	5.1	-5 5 -5	18.1	-19.0	-3	11.8	-12.2	-3	16.4	17.0
3 3 -6	0.0	-1.6	4	9.7	-11.6	4	-2	11.6	-2	6.0	-8.2	-2	13.6	15.2
-5	26.5	30.1	5	19.5	-19.4	-1	9.9	-8.8	-1	6.6	-10.0	-1	8.9	-10.1
-4	7.2	7.0	0 4 -7	7.8	7.3	0	17.6	-18.1	0	34.9	32.6	2	38.5	37.4
-3	59.6	58.5	-6	17.9	18.7	-4 5 -5	2.2	2.8	1	74.2	-67.9	3	40.3	-37.8
-2	22.6	25.0	-5	0.0	0.9	-4	17.7	18.8	2	93.9	-89.5	4	4.3	-1.0
-1	25.5	26.5	-4	42.5	42.6	-3	9.8	-9.9	3	10.7	-11.3	5	1.5	0.0
0	22.9	22.3	-3	9.5	-9.9	-2	0.8	-1.0	4	19.7	-16.9	6	7.0	8.0
1	3.8	-5.5	-2	81.3	-82.2	-1	16.1	-18.9	5	3.6	-5.8	3 6 -5	23.4	24.3
2	41.0	42.5	-1	0.4	7.1	0	19.8	21.2	6	17.1	-17.5	0	13.7	15.6
3	65.9	-67.3	0	10.3	-12.6	1	14.9	-16.9	7	13.6	16.4	-3	47.5	46.3
4	29.9	-32.4	1	19.4	22.4	2	54.4	-52.2	5 5 -4	1.3	0.4	-2	10.3	11.8
5	9.2	-11.3	2	36.6	-40.9	-3 5 -6	9.6	9.5	-3	7.8	7.2	-1	7.7	7.0
6	7.8	9.3	3	17.5	17.5	-5	2.8	-2.9	-2	23.5	23.8	0	11.1	9.3
7	11.9	-14.0	4	26.4	28.4	4	5.1	4.5	1	30.8	31.6	2	26.6	23.5
4 3 -5	17.1	-19.4	5	14.6	-15.3	-3	8.6	-11.6	0	26.3	26.0	3	7.5	-4.0
-4	21.2	24.0	6	14.5	-14.4	-2	21.3	20.9	1	1.9	-1.2	4	8.7	-8.9
-3	3.5	-4.8	1 4 -6	6.2	5.8	-1	2.5	0.1	2	7.7	7.1	5	14.0	14.0
-2	45.0	-48.8	-5	5.1	1.6	0	1.9	4.8	3	5.5	7.1	6	4.1	3.7
-1	50.7	44.3	-4	45.4	45.6	1	4.4	4.8	4	21.7	-20.8	4 6 -5	10.8	-11.5
0	14.1	13.7	-3	16.2	-17.8	2	9.1	-11.5	5	18.6	-18.4	-4	3.5	-0.3
1	31.8	32.1	-2	26.0	26.4	3	5.2	-3.9	6	36.9	-38.5	-3	2.0	0.9
2	4.6	-3.6	-1	11.9	10.4	4	8.2	-7.8	6 5 -3	21.2	-22.2	-2	27.7	-28.1
3	4.4	6.3	1	44.2	-44.4	-2 5 -6	3.0	-4.3	-2	24.5	26.0	-1	50.9	51.1
4	43.0	46.9	2	86.0	-82.9	-1	60.8	-67.0	0	25.1	-27.1	0	33.5	29.6
5	28.6	-31.3	3	22.4	23.1	-4	32.9	-31.4	0	11.3	12.2	1	17.8	-16.2
6	27.7	-25.9	4	48.4	49.9	-3	14.0	-12.4	1	38.4	39.5	2	12.7	9.5
7	3.9	1.2	5	5.3	-4.6	-2	36.6	35.6	2	48.5	49.0	3	7.8	-8.0
5 3 -4	9.2	-9.3	6	14.9	14.6	-1	12.1	-11.2	3	23.3	23.0	4	28.2	26.3
-2	35.9	-39.5	7	14.0	15.0	0	5.1	5.0	-4	8.5	-9.7	5	16.6	-17.1
-1	13.3	-14.7	2 4 -6	5.9	-4.2	1	39.9	40.3	5	26.1	25.4	6	9.5	-10.3
0	20.3	-22.7	-5	8.3	-9.4	2	27.6	27.4	6	8.8	7.8	5 6 -4	0.9	-1.0
1	29.8	30.4	-4	35.6	-36.2	3	20.0	18.6	7 5 -1	29.9	-30.2	-3	18.1	-17.6
2	35.3	-39.7	-3	15.2	-15.9	4	8.9	-10.6	0	8.2	-8.0	-2	17.5	-16.2
3	9.3	8.5	-2	86.0	87.9	5	13.5	13.0	1	20.0	-19.9	-1	18.1	16.9
4	18.3	20.4	-1	37.3	-41.2	-1 5 -6	21.1	-21.5	2	16.9	18.0	0	27.3	-24.5
5	17.4	-20.2	0	39.5	-35.6	-5	10.8	10.7	3	8.6	-9.2	1	21.6	19.9
6	11.2	14.0	1	4.0	5.0	-4	38.7	-38.9	4	5.6	-4.6	2	39.9	-36.7
7	8.1	-8.9	2	11.6	11.5	-3	5.6	4.0	-4 6 -4	8.5	9.1	3	4.7	3.3
6 3 -3	4.7	2.2	3	8.2	8.7	-2	25.9	-28.0	-1	9.9	10.4	4	21.5	18.4
-2	6.1	7.6	4	82.4	-85.3	-1	22.1	-20.9	-2	22.1	-24.1	5	24.5	-22.6
-1	19.5	-21.7	5	29.1	29.8	0	15.3	14.6	-1	45.5	43.2	6	4.2	3.9
0	43.2	-46.5	6	13.4	14.5	1	31.7	-32.1	0	21.3	21.8	-2	15.1	15.2
1	7.0	-7.7	7	2.8	3.0	2	54.4	54.2	1	25.8	25.6	-2	18.6	17.0
2	4.6	4.6	3 4 -6	16.8	-17.4	3	7.5	-7.3	-3 6 -5	25.1	-22.8	-1	26.2	-25.8
3	6.2	10.4	-5	10.1	-10.8	4	10.1	11.7	-4	2.0	-2.5	0	24.7	-24.9
4	19.1	-21.1	-4	14.1	-14.4	5	32.1	33.1	-3	19.2	-20.3	1	2.8	1.2
6	5.0	4.9	-3	8.6	-7.5	6	23.8	22.4	-2	13.0	-14.4	2	10.9	11.7
7 3 -0	7.3	8.4	-2	5.7	-5.4	0 5 -6	4.9	-3.5	-1	5.4	-6.1	3	3.3	-4.2
0	8.7	-11.5	-1	0.0	-0.3	-5	19.2	19.6	0	15.6	-17.1	4	21.7	-20.4
2	6.1	7.5	0	32.0	32.2	-4	49.6	51.3	1	12.4	15.2	5	9.9	9.5
3	7.3	-8.5	1	16.3	15.7	-3	3.2	1.8	2	18.1	-20.0	7 6 -1	3.4	1.7
4	4.8	-3.3	2	35.2	35.0	-2	65.4	-66.2	-3	11.6	11.9	0	5.5	6.3
5	5.2	7.0	3	34.1	-33.7	-1	1.5	5.3	-2 6 -5	12.0	12.4	1	8.2	9.1
-5 4 -4	12.7	-15.5	4	20.7	-19.8	0	2.7	-0.7	-4	0.0	-1.3	2	8.7	-9.3
-3	5.4	-7.5	5	10.8	10.5	1	18.2	-19.3	-3	7.0	-6.2	3	13.1	-15.7
0	4.2	9.2	6	15.9	-15.6	2	26.9	-29.0	-2	26.2	26.8	4	18.2	-20.9
1	0.0	-3.7	7	8.3	-10.8	3	22.5	-21.6	-1	18.3	-20.3	-3 7 -4	1.7	-3.0
-4 4 -6	29.9	-28.1	4 4 -5	0.0	0.4	4	29.1	29.1	0	40.4	-40.1	-3	10.4	10.8
-5	18.8	17.2	-4	27.7	27.9	5	29.4	-28.6	1	21.3	-22.0	-2	2.2	0.4
-4	1.7	1.0	-3	5.1	-6.2	6	22.6	-20.8	2	16.8	-15.1	-1	4.1	1.8
-3	3.1	-3.7	-2	6.1	4.8	1 5 -6	10.2	10.4	3	0.0	-1.7	0	15.6	17.5
-2	21.1	-26.3	0	34.7	33.9	-5	14.2	16.1	4	38.2	-37.1	1	18.8	-20.6
3	0.0	1.1	1	6.4	7.2	-4	3.3	3.6	-1 6 -6	5.6	5.3	2	5.4	-5.1
-3 4 -6	18.0	19.8	2	13.4	-14.0	-3	24.5	27.0	-4	32.6	31.6	-2 7 -5	24.7	-24.0
-5	46.7	47.0	3	26.1	26.3	-2	46.1	43.2	-3	8.3	0.7	-4	21.3	-20.3
-4	6.3	-9.5	4	51.3	52.0	-1	51.4	53.6	-2	27.9	27.4	-3	20.1	20.4
-3	21.1	20.7	5	12.0	12.6	1	6.1	5.7	-1	21.7	22.4	-2	16.4	16.9
-2	2.5	-0.8	6	9.2	-10.2	2	11.3	-12.1	1	24.1	26.0	-1	22.8	24.7
0	2.9	3.9	7	6.6	5.3	3	7.6	-6.6	2	6.0	-7.1	0	35.7	-31.1
1	43.3	42.4	5 4 -4	25.1	-24.5	4	0.0	-2.7	3	26.3	-25.3	1	0.8	3.4
2	24.1	-22.2	-3	14.6	16.2	5	47.0	-45.9	4	35.7	-35.1	2	22.9	25.2
3	14.5	15.4	-2	31.5	-33.6	6	17.0	-18.1	5	11.0	-9.0	3	13.6	-25.8
4	5.8	-7.7	-1	13.3	15.2	2 5 -6	27.9	28.8	0 6 -6	41.0	-39.2	-1 7 -5	24.6	-12.6
5	0.0	1.5	0	27.9	29.6	-5	40.0	-41.6	-5	8.8	-8.6	-4	4.2	-3.5
-2 4 -7	25.2	-23.4	1	32.8	-33.2	-4	19.7	-19.9	0	12.8	-12.5	-4	21.0	-20.3
-6	25.7	24.1	2	15.2	15.9	-3	22.1	22.1	-3	42.8	-42.5	-2	10.9	-10.1
-5	17.8	-18.2	3	5.8	-7.7	-2	16.5	16.1	-1	8.1	-7.6	-1	21.2	24.9
-4	27.9	-27.9	4	27.1	27.8	1	30.6	31.2	0	41.4	38.7	0	17.1	-18.6
-3	24.9	25.0	5	5.4	-8.6	2	51.5	51.0	1	16.2	17.5	1	40.8	35.3
-2	44.2	45.1	6	8.9	-10.4	3	2.7	-2.5	2	11.6	-14.2	2	9.5	8.9
-1	41.8	43.1	7	47.6	48.0	4	19.4	17.3	3	46.8	47.6	3	11.1	-11.7
0	34.0	32.8	0	23.9	25.5	5	13.9	13.4	4	9.0	8.8	4	5.5	-5.3
1	33.5	34.5	-1	5.3	4.6	6	9.5	9.7	5	4.1	3.9	0 7 -5	6.3	1.8
2	22.5	-20.5	-2	36.3	-38.1	7	16.7	-17.3	-6	14.8	-15.1	-4	20.7	20.7
3	8.8	-9.8	1	5.3	-5.8	-3	24.2	-24.8	-5	1.9	-1.3	-2	27.9	-28.7
4	14.0	-16.9	2	34.1	37.0	-2	39.2	-40.1	-4	39.6	-41.5	1	2.8	0.2
-1 4 -7	2.0	0.2	3	52.8	-55.8	-1	16.7	-17.7	-3	2.3	-2.7	3	1.8	2.9
-6	16.8	-16.9	4	19.4	-21.5	0	86.0	-78.6	-2	52.2	-52.7	4	21.1	22.2
-5	24.3	-23.6	5	19.1	-21.6	1	32.4	-27.7	-1	32.8	-31.5	5	8.0	6.6
			6	0.0	1.3	2	9.1	-7.9	2	19.2				

Table 3. (Continued)

h k l	$ F_o $	$F_c$	h k l	$ F_o $	$F_c$	h k l	$ F_o $	$F_c$	h k l	$ F_o $	$F_c$	h k l	$ F_o $	$F_c$
1 7 -3	6.7	-8.1	2 7 4	57.5	-58.1	4 7 -4	8.7	7.7	5 7 -2	6.6	-6.6	6 7 2	13.8	14.5
-2	9.5	-10.2	5	6.5	-4.5	-3	3.1	-3.4	-1	16.5	-15.0	3	40.5	-41.5
2	35.6	-33.6	6	5.5	5.9	-2	23.7	-23.2	0	23.8	23.7	4	10.8	-10.7
3	13.2	14.2	3 7 -4	6.1	-5.4	-1	5.5	-3.1	1	39.5	-37.2	5	4.9	-4.7
4	19.5	21.6	-2	8.2	6.7	0	27.5	23.8	2	9.1	-8.4	7 7 1	32.5	32.4
5	8.9	-9.0	-1	6.9	-6.0	1	9.5	-9.5	3	10.8	11.4	2	9.4	8.2
2 7 -5	5.2	-5.0	2	28.2	24.5	2	12.7	11.9	4	7.7	7.6	3	2.6	-2.9
-4	6.8	-8.7	3	4.9	4.1	3	13.5	13.6	5	14.1	15.3			
-3	18.1	-17.6	4	28.4	-28.7	4	44.2	46.5	6 7 -1	3.5	3.0			
-2	42.4	39.3	5	19.4	21.2	5	15.8	15.6	0	15.7	-14.7			
3	5.3	-5.7	6	15.0	-17.9	6	0.0	-0.7	1	14.5	-13.5			

a volume of 0.0005 mm<sup>3</sup> was found. Nickel-filtered CuK $\alpha$  radiation was used to measure 1051 reflections with an equi-inclination single-crystal diffractometer. The diffracted x-ray beams were recorded by a proportional counter connected with a pulse-height discriminator. The integrated intensities were corrected for Lorentz and polarization factors as well as for absorption. The observed structure factors are listed in Table 3.

### Structure determination and refinement

A three-dimensional Patterson function was computed. In order to interpret it, all its maxima were projected along the  $a$  axis. A careful investigation of this map showed that the high peaks outline a subcell with one third of the volume of the original cell. The transformation of the original cell vectors to those for the subcell is as follows:

$$\begin{aligned} a' &= a \\ b' &= \frac{1}{3}b - \frac{1}{3}c \\ c' &= c. \end{aligned}$$

About 300 reflections with indices  $hkl$  corresponding to the subcell were selected from the full data deck. These 300 strong reflections were used to compute a Patterson function which, projected along  $a$ , is shown schematically in Fig. 1a. Figure 1b illustrates a substructure model containing two possible locations of heavy atoms which are derived from the Patterson map seen in Fig. 1a. If three of these substructure cells are arranged in such a way that they cover the same volume as the true cell of high-pressure CaSiO<sub>3</sub>, six independent positions for the metal atoms are obtained. These atomic positions were tested on a set of reflection amplitudes with  $|F_{\text{obs}}| > 30$ , which represents roughly half of the whole reflection set. The structure-factor computation yielded an  $R$  value of 44%, thus warranting considering this proposal as a possible candidate for the structure of this high-pressure phase of CaSiO<sub>3</sub>.

Further evidence supporting these findings was obtained by reiterative application of SAYRE's (1952) equation. This was performed with an IBM 7094 program REL written by R. E. LONG, University of California, Los Angeles. The sign determination was carried out on 181 reflections each of which had a normalized structure factor  $|E| > 1.4$ . This resulted in four alternative models which were found to have reasonable interatomic distances between the metal atoms. In LONG's program the quality of a result can be appraised by the number of cycles required to reach consistency in the prediction of signs and a consistency index. This index expresses the average

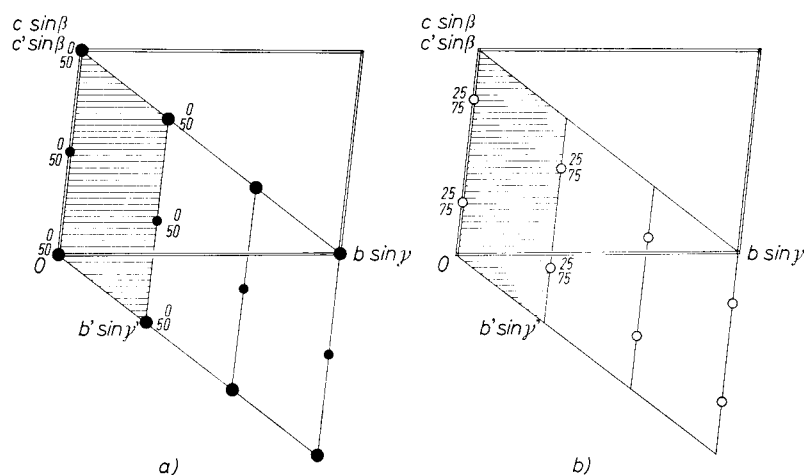


Fig. 1. Schematic presentation of the substructure of high-pressure  $\text{CaSiO}_3$ . The subcell is shaded, the true cell is outlined by double lines. The numbers give the heights  $x$  in hundredths. (a) Idealized substructure Patterson projected along  $a$ , showing only the high peaks. (b) Idealized substructure model derived from the Patterson map shown in Fig. 1a

change in sign within a given set of reflections and is normalized so that its limits are 0 and 1. Usually the true solution has a consistency index approaching the upper limit and a small number of cycles. A study of these models revealed that the one with the highest consistency index = 0.971, and the lowest number of cycles was almost identical with the proposal obtained by analysis of the Patterson map of the subcell.

Accordingly a Fourier synthesis based on the six positions of the metal atoms was computed. This function produced additional peaks

which could be interpreted as the locations of the nine oxygen atoms. Employing the positional parameters of the six metal atoms and the nine oxygen atoms, a structure-factor computation gave an  $R$  value of 30%, suggesting that the preliminary atomic coordinates were probably correct.

Figure 2 illustrates the close resemblance of the proposed arrangement of the metal atoms to the actual location of these atoms as obtained during a later stage of the investigation. A preliminary cycle of least-squares refinement of these positional parameters, using

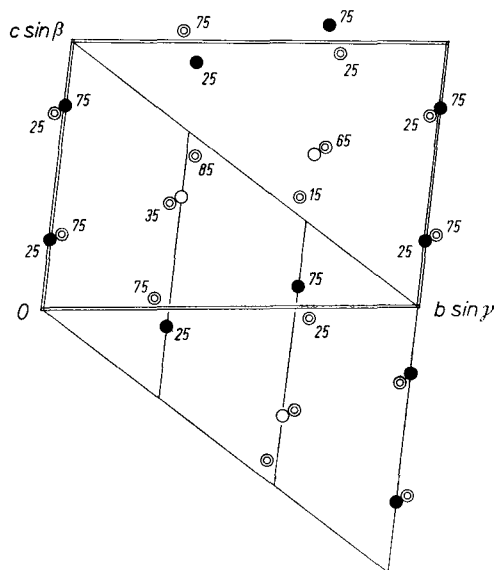


Fig. 2. Comparison of the atomic positions suggested by the substructure with the actual locations of the Ca and Si atoms. The black full circles represent atoms with no deviation from the predicted position. The double circles represent atoms which do not quite correspond to the positions derived from the substructure (empty circles). The numbers give the heights  $z$  in hundredths. The true cell is outlined by double lines

equal weights and an overall isotropic temperature factor of  $B = 1.0 \text{ \AA}^2$ , decreased the  $R$  value from 30% to 20%. In continuing the refinement, a weighting scheme was introduced based on a weighting factor  $w = |F_{\text{obs}}|$ , described by DE VRIES (1965). When all parameters were allowed to vary, the best  $R$  value with isotropic temperature factors was 9.4% and with anisotropic thermal parameters, 6.5%.

### Discussion of the structure

The basic structural features of this high-pressure phase of  $\text{CaSiO}_3$  are  $\text{CaO}$  layers and  $\text{Si}_3\text{O}_9$  rings. The layers contain two types of Ca atoms, one coordinated by six oxygen atoms the other by eight oxygen atoms. The  $\text{Si}_3\text{O}_9$  rings are located between these layers. The third type of Ca atom, also coordinated by six oxygen atoms, connects neighboring layers, thus sharing the space with the  $\text{Si}_3\text{O}_9$  rings. The rings are seen projected along  $a$  in Fig. 3. The Ca layers and their orientation with respect to the cell of high-pressure  $\text{CaSiO}_3$  are illustrated in Fig. 8a.

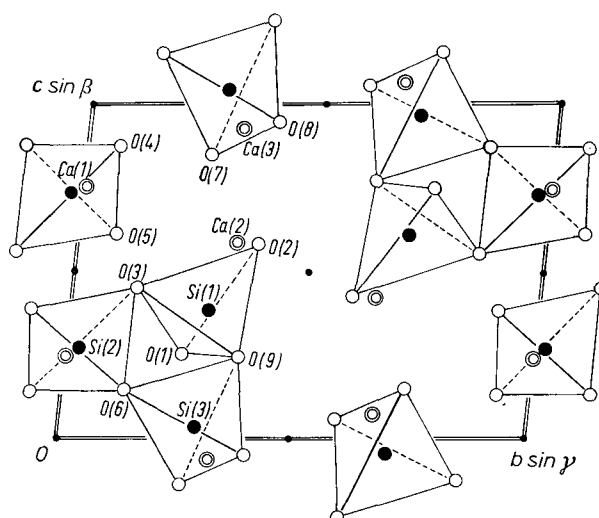


Fig. 3. Projection along  $a$  of the structure of high-pressure  $\text{CaSiO}_3$ . The double circles are Ca atoms, the full circles Si atoms, and the single circles O atoms

All atoms in this structure occupy the general position  $2i$  in space group  $P\bar{1}$ . The refined coordinates are listed in Table 4. Table 5 gives the interatomic distances and Table 6 the bond angles between atoms.

The cell of high-pressure  $\text{CaSiO}_3$  contains three  $\text{CaO}$  layers as seen in Fig. 8a. The Ca atoms define planes parallel to  $(111)$  which intersect the axes at  $\frac{1}{2}$ . A view normal to the  $\text{CaO}$  layer is illustrated in Fig. 4. If the  $\text{Ca}(2)$  octahedra, which are not located within the layer, are neglected Fig. 4 shows that the layer is composed of oxygen polyhedra around  $\text{Ca}(1)$  and  $\text{Ca}(3)$  which share edges with each other. These polyhedra do not fill all the space of the layer, which has large voids. The  $\text{Ca}(2)$  octahedra, shown lightly in Fig. 4, are above and

Table 4. Atomic coordinates for the high-pressure polymorph of CaSiO<sub>3</sub>

Atom	<i>x</i>	$\sigma(x)$	<i>y</i>	$\sigma(y)$	<i>z</i>	$\sigma(z)$
Ca(1)	0.7441	0.0003	0.0002	0.0003	0.7623	0.0003
Ca(2)	0.8789	0.0003	0.3513	0.0003	0.5846	0.0003
Ca(3)	0.2443	0.0003	0.3356	0.0003	0.9245	0.0003
Si(1)	0.3684	0.0004	0.2951	0.0004	0.3916	0.0004
Si(2)	0.7583	0.0004	0.0162	0.0004	0.2701	0.0004
Si(3)	0.7218	0.0004	0.3009	0.0004	0.0416	0.0004
O(1)	0.2150	0.0010	0.2564	0.0009	0.2656	0.0009
O(2)	0.2140	0.0009	0.4055	0.0008	0.5843	0.0009
O(3)	0.5556	0.0010	0.1359	0.0009	0.4518	0.0009
O(4)	0.3391	0.0010	0.0612	0.0009	0.8715	0.0010
O(5)	0.0629	0.0010	0.0932	0.0009	0.6140	0.0010
O(6)	0.8661	0.0010	0.1386	0.0009	0.1353	0.0010
O(7)	0.6282	0.0010	0.2629	0.0009	0.8591	0.0009
O(8)	0.8650	0.0010	0.4031	0.0009	0.9540	0.0010
O(9)	0.5154	0.0010	0.3853	0.0009	0.2426	0.0009

Table 5. Interatomic distances

Atoms with a primed number are equivalent by symmetry to atoms of the same number without primes

Atoms	Distance	$\sigma$	Atoms	Distance	$\sigma$
Ca(1)–O(1')	2.314 Å	0.009 Å	Ca(2)–O(1'')	2.637 Å	0.006 Å
Ca(1)–O(3)	2.709	0.007	Ca(2)–O(2')	2.412	0.007
Ca(1)–O(4)	2.506	0.007	Ca(2)–O(2'')	2.458	0.006
Ca(1)–O(4')	2.446	0.007	Ca(2)–O(5')	2.314	0.008
Ca(1)–O(5')	2.529	0.007	Ca(2)–O(7)	2.472	0.007
Ca(1)–O(5'')	2.580	0.007	Ca(2)–O(8)	2.510	0.007
Ca(1)–O(6')	2.725	0.007	Average	2.467	
Ca(1)–O(7)	2.368	0.008	Si(2)–O(3)	1.701	0.007
Average	2.630		Si(2)–O(4''')	1.589	0.007
Ca(3)–O(1)	2.329	0.007	Si(2)–O(5'')	1.609	0.007
Ca(3)–O(2)	2.358	0.006	Si(2)–O(6)	1.652	0.008
Ca(3)–O(4)	2.426	0.009	Average	1.638	
Ca(3)–O(7)	2.364	0.006	Si(3)–O(6)	1.669	0.008
Ca(3)–O(8)	2.363	0.007	Si(3)–O(7')	1.600	0.007
Ca(3)–O(8')	2.409	0.008	Si(3)–O(8''')	1.558	0.008
Average	2.375		Si(3)–O(9)	1.681	0.007
Si(1)–O(1)	1.607	0.007	Average	1.627	
Si(1)–O(2)	1.603	0.007			
Si(1)–O(3)	1.683	0.008			
Si(1)–O(9)	1.626	0.007			
Average	1.630				

Table 6. *Bond angles*

Atoms with a primed number are equivalent by symmetry to atoms of the same number without primes

Atoms	Angle	Atoms	Angle
O(4)—Ca(1)—O(5')	148° 06'	O(3)—Si(2)—O(6)	100° 56'
O(1')—Ca(1)—O(4')	79° 54'	O(4''')—Si(2)—O(3)	110° 56'
O(1')—Ca(1)—O(5'')	71° 30'	O(4''')—Si(2)—O(5'')	118° 29'
O(5'')—Ca(1)—O(3)	60° 37'	O(4''')—Si(2)—O(6)	110° 08'
O(3)—Ca(1)—O(7)	78° 28'	O(5'')—Si(2)—O(3)	107° 37'
O(7)—Ca(1)—O(6')	72° 45'	O(5'')—Si(2)—O(6)	107° 11'
O(4')—Ca(1)—O(6')	73° 21'		
		O(6)—Si(3)—O(7')	109° 58'
O(2'')—Ca(2)—O(7)	131° 40'	O(6)—Si(3)—O(8''')	111° 14'
O(5')—Ca(2)—O(1'')	70° 25'	O(6)—Si(3)—O(9)	104° 40'
O(1'')—Ca(2)—O(2'')	61° 11'	O(7')—Si(3)—O(8''')	108° 16'
O(2'')—Ca(2)—O(8)	73° 20'	O(8''')—Si(3)—O(9)	112° 39'
O(5')—Ca(2)—O(8)	91° 10'	O(9)—Si(3)—O(7')	110° 01'
O(7)—Ca(3)—O(8)	174° 11'	Si(1)—O(3)—Si(2)	122° 56'
O(1)—Ca(3)—O(4)	79° 59'	Si(1)—O(9)—Si(3)	123° 20'
O(4)—Ca(3)—O(2)	96° 41'	Si(3)—O(6)—Si(2)	124° 03'
O(4)—Ca(3)—O(8)	97° 37'		
O(1)—Ca(3)—O(8)	92° 34'	O(3)—O(6)—O(9)	59° 23'
		O(3)—O(9)—O(6)	59° 03'
O(1)—Si(1)—O(2)	108° 03'	O(6)—O(3)—O(9)	61° 34'
O(1)—Si(1)—O(3)	112° 23'		
O(1)—Si(1)—O(9)	108° 55'	Si(1)—Si(3)—Si(2)	61° 10'
O(2)—Si(1)—O(9)	108° 43'	Si(2)—Si(1)—Si(3)	59° 47'
O(3)—Si(1)—O(2)	115° 10'	Si(3)—Si(2)—Si(1)	59° 03'
O(3)—Si(1)—O(9)	130° 19'		

below the layer. Ca(1) is coordinated by eight oxygen atoms forming a distorted scalenohedron. The largest Ca—O distance within this polyhedron is 2.725 Å, which lies between similar unusually large Ca—O distances found by PREWITT and BUEGER (1963) for wollastonite:  $\text{Ca}_3\text{—O}_9 = 2.642$  Å; and by TROJER (1968) for parawollastonite:  $\text{Ca}(1)\text{—O}(9) = 2.895$  Å. Ca(3) has octahedral coordination with an average Ca—O distance of 2.375 Å.

Each layer is connected with the neighboring layers both by  $\text{Si}_3\text{O}_9$  rings and by two Ca(2) octahedra which are located above and below each layer. In Fig. 5, centrosymmetrically related parts of two neighboring layers are shown. The polyhedra to the right (light shading) are part of the same layer illustrated in Fig. 4. The polyhedra to the left (dark shading) belong to the centrosymmetrical layer

below. A pair of Ca(2) octahedra (cross-hatched) links those two layers. This connection can be described as follows: The Ca(2) octahedron on the right shares two edges with two Ca(1) polyhedra belonging to the layer above. The same octahedron also shares corners with two Ca(3) octahedra of the layer above and shares a corner with one Ca(3) octahedron in the layer below. The other Ca(2) octahedron on the left is linked up in a centrosymmetrical way. The two Ca(2) octahedra themselves share an edge with each other. The coordination octahedron around Ca(2) is highly distorted so that the average

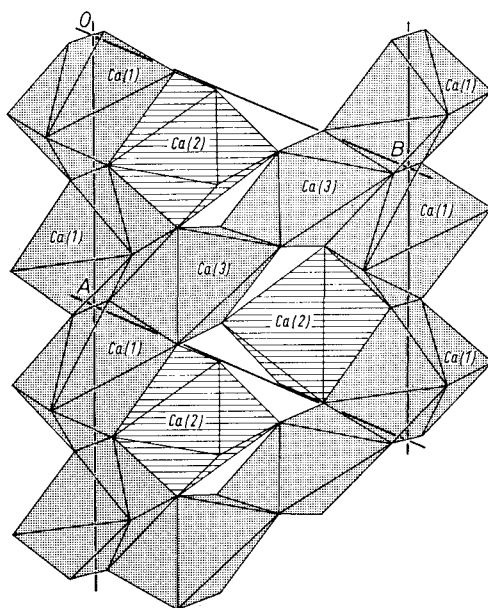


Fig. 4. The Ca—O layer. The Ca(1) and Ca(3) polyhedra within the layer have dark shading. The Ca(2) octahedra (hatched), actually above and below the layer, are projected onto the layer

Ca—O distances, 2.467 Å, is larger than the one for the more regular Ca(3) coordination polyhedron which has an average Ca—O distance of 2.375 Å.

As pointed out before, the Ca(1) and Ca(3) polyhedra form an incomplete layer. In Fig. 4 the Ca(2) octahedra, actually located above and below the layer, are projected onto the layer. As seen in this figure, these octahedra fit the voids of the layer very well. Thus it would be geometrically possible to obtain a layer of linked polyhedra by stuffing the Ca(2) octahedra next to Ca(3). Only minor distortions

of the Ca(2) octahedra would be necessary to make them share edges with their neighboring polyhedra. The result would be a distorted but complete layer composed of oxygen octahedra and scalenohedra sharing edges with each other.

The Si atoms are tetrahedrally coordinated by oxygen atoms. The tetrahedra share corners to form three-member rings, seen in Fig. 3, which are located between the layers and next to Ca(2). A schematic presentation of this arrangement is given in Fig. 6. This shows that two rings in the central interlayers space are separated by a pair of

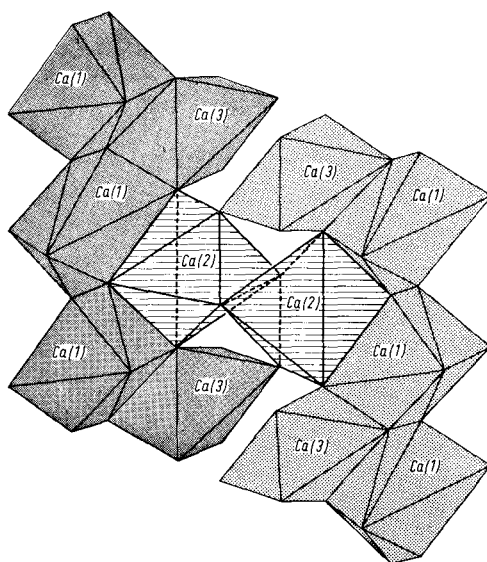


Fig. 5. Graphic presentation of the Ca(2) octahedra connecting two parts of neighboring layers. The polyhedra on the right with light shading are part of the same layer illustrated in Fig. 4. The polyhedra on the left have dark shading and are part of the layer below. The Ca(2) octahedra are hatched

Ca(2) octahedra. The  $\text{Si}_3\text{O}_9$  rings are rather compact units with only minor distortions, as seen in Fig. 7. The average Si—O distances are roughly equal: Si(1)—O = 1.630 Å, Si(2)—O = 1.638 Å, and Si(3)—O = 1.627 Å. The deviation from the ideal tetrahedral angle,  $109^\circ 28'$ , does not exceed  $11^\circ 11'$ . This is a relative small discrepancy if compared with a deviation of  $20^\circ 02'$  reported by TROJER (1968) for parawollastonite. The silicon atoms within a  $\text{Si}_3\text{O}_9$  group form an equilateral triangle to good approximation as seen from the bond angles listed in Table 6.

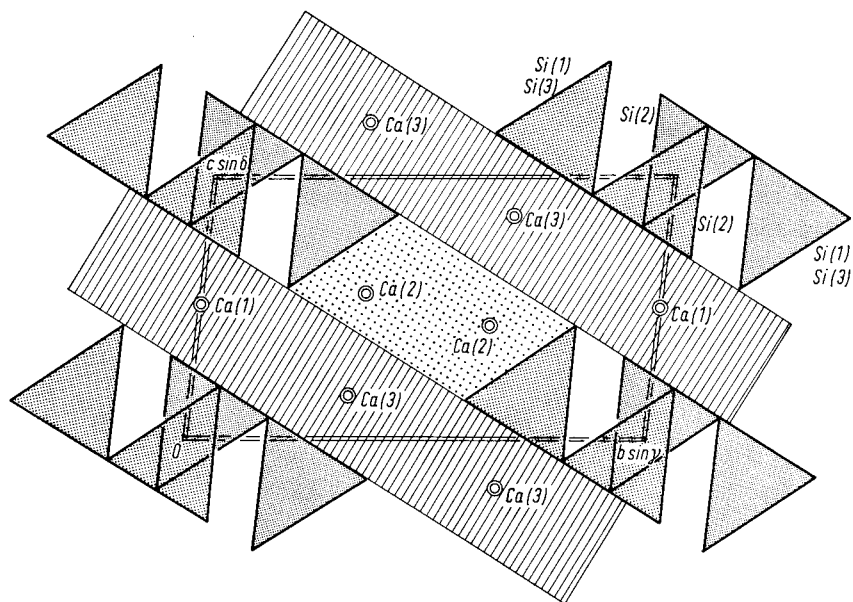


Fig. 6. Schematic projection parallel (101). The Si<sub>3</sub>O<sub>9</sub> rings and the Ca(2) octahedra are located between the layers composed of Ca(1) and Ca(3). The layers are hatched, the Ca(2) octahedra have light shading, and the rings have dark shading.  $\delta$  is the acute angle between the planes (100) and (101)

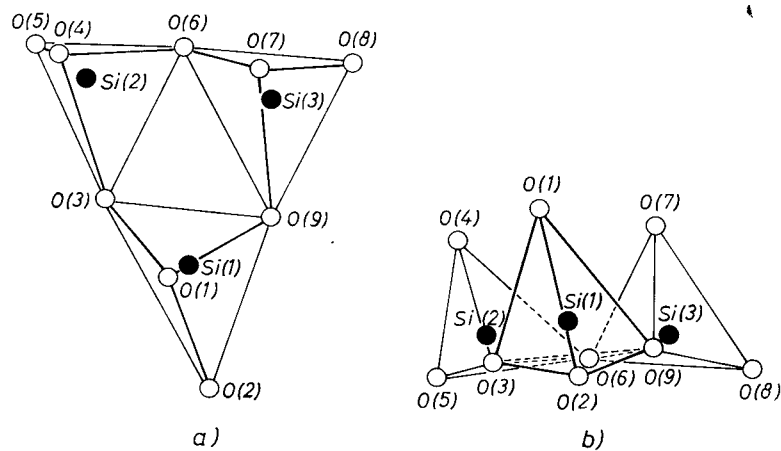


Fig. 7. A silicon-oxygen ring. (a) Projected along  $C$ ; (b) viewed parallel to the Ca plane

The anisotropic temperature coefficients for this high-pressure phase of CaSiO<sub>3</sub> are found in Table 7. The thermal parameters are listed in Table 8. The  $q_i$ 's are the three principal axes of the thermal-

Table 7. *Anisotropic temperature coefficients*

Atoms	$\beta_{11}$	$\beta_{22}$	$\beta_{33}$	$\beta_{12}$	$\beta_{13}$	$\beta_{23}$
Ca(1)	0.0059	0.0062	0.0029	-0.0024	-0.0008	0.0005
$\sigma$	0.0006	0.0004	0.0004	0.0003	0.0004	0.0003
Ca(2)	0.0047	0.0065	0.0048	-0.0016	-0.0007	0.0000
$\sigma$	0.0005	0.0004	0.0004	0.0004	0.0004	0.0003
Ca(3)	0.0048	0.0064	0.0023	-0.0019	-0.0014	-0.0002
$\sigma$	0.0005	0.0004	0.0004	0.0003	0.0003	0.0003
Si(1)	0.0023	0.0060	0.0023	-0.0010	-0.0003	-0.0008
$\sigma$	0.0007	0.0005	0.0005	0.0004	0.0005	0.0004
Si(2)	0.0048	0.0051	0.0024	-0.0016	-0.0011	-0.0006
$\sigma$	0.0007	0.0005	0.0006	0.0005	0.0005	0.0004
Si(3)	0.0050	0.0063	0.0019	-0.0018	-0.0006	-0.0004
$\sigma$	0.0007	0.0005	0.0006	0.0005	0.0005	0.0004
O(1)	0.0038	0.0110	0.0038	-0.0035	-0.0030	0.0013
$\sigma$	0.0019	0.0015	0.0015	0.0015	0.0013	0.0011
O(2)	0.0018	0.0044	0.0040	0.0000	-0.0001	-0.0009
$\sigma$	0.0016	0.0012	0.0015	0.0011	0.0012	0.0010
O(3)	0.0106	0.0067	0.0039	-0.0057	-0.0024	0.0004
$\sigma$	0.0021	0.0014	0.0015	0.0013	0.0013	0.0011
O(4)	0.0062	0.0096	0.0053	-0.0045	-0.0047	0.0009
$\sigma$	0.0020	0.0015	0.0016	0.0013	0.0014	0.0011
O(5)	0.0067	0.0073	0.0067	-0.0026	0.0033	0.0004
$\sigma$	0.0019	0.0014	0.0017	0.0012	0.0014	0.0011
O(6)	0.0059	0.0074	0.0094	-0.0036	-0.0037	0.0005
$\sigma$	0.0020	0.0014	0.0017	0.0013	0.0014	0.0011
O(7)	0.0055	0.0100	0.0034	-0.0039	-0.0024	-0.0005
$\sigma$	0.0019	0.0015	0.0016	0.0013	0.0013	0.0011
O(8)	0.0057	0.0048	0.0034	-0.0019	-0.0021	0.0000
$\sigma$	0.0019	0.0013	0.0016	0.0012	0.0013	0.0010
O(9)	0.0038	0.0078	0.0022	-0.0021	0.0004	0.0002
$\sigma$	0.0019	0.0014	0.0015	0.0012	0.0013	0.0010

vibration ellipsoid. To each magnitude  $q_i$  there corresponds a temperature factor  $B_i$  along a principal axis  $i$ . An average temperature factor  $B$  is defined by  $B = (B_1 + B_2 + B_3)/3$ , which is comparable to the regular isotropic temperature factor; this is given in the last

Table 8. *Thermal parameters*

Atom	$q_1$	$B_1$	$q_2$	$B_2$	$q_3$	$B_3$	Equivalent isotropic $B$
Ca(1)	0.110 Å	0.95 Å <sup>2</sup>	0.161 Å	2.06 Å <sup>2</sup>	0.078 Å	0.48 Å <sup>2</sup>	1.16 Å <sup>2</sup>
σ	0.005	0.08	0.005	0.13	0.006	0.07	0.05
Ca(2)	0.091	0.65	0.167	2.19	0.108	0.92	1.25
σ	0.004	0.06	0.005	0.12	0.003	0.05	0.05
Ca(3)	0.097	0.74	0.164	2.13	0.070	0.39	1.08
σ	0.005	0.08	0.005	0.12	0.006	0.07	0.05
Si(1)	0.081	0.52	0.160	2.01	0.059	0.28	0.94
σ	0.006	0.08	0.007	0.17	0.007	0.07	0.07
Si(2)	0.096	0.73	0.147	1.70	0.072	0.41	0.95
σ	0.007	0.10	0.007	0.16	0.010	0.11	0.07
Si(3)	0.100	0.79	0.164	2.12	0.063	0.31	1.07
σ	0.007	0.11	0.007	0.17	0.009	0.09	0.07
O(1)	0.074	0.43	0.213	3.58	0.090	0.64	1.55
σ	0.020	0.23	0.017	0.56	0.016	0.23	0.21
O(2)	0.042	0.36	0.139	1.54	0.095	0.71	0.87
σ	0.035	0.25	0.018	0.39	0.016	0.24	0.17
O(3)	0.142	1.60	0.162	2.06	0.092	0.67	1.11
σ	0.014	0.34	0.017	0.44	0.017	0.25	0.19
O(4)	0.093	0.68	0.196	3.04	0.114	1.02	1.58
σ	0.013	0.19	0.015	0.47	0.012	0.21	0.15
O(5)	0.113	1.00	0.174	2.39	0.120	1.13	1.51
σ	0.016	0.29	0.016	0.43	0.014	0.27	0.19
O(6)	0.105	0.87	0.174	2.38	0.133	1.40	1.55
σ	0.018	0.29	0.016	0.45	0.013	0.28	0.20
O(7)	0.102	0.83	0.201	3.18	0.084	0.56	1.52
σ	0.017	0.28	0.014	0.46	0.019	0.25	0.19
O(8)	0.103	0.84	0.144	1.63	0.118	1.10	1.19
σ	0.016	0.25	0.018	0.40	0.014	0.26	0.18
O(9)	0.094	0.70	0.181	2.59	0.063	0.32	1.20
σ	0.016	0.24	0.016	0.45	0.020	0.20	0.18

column of this table. The temperature factors found in this crystal structure are slightly higher than those published for wollastonite by BUERGER and PREWITT (1961).

## Comparison with related structures

GLASSER and GLASSER (1961) determined the structure of walstromite, Ca<sub>2</sub>BaSi<sub>3</sub>O<sub>9</sub>, which is chemically similar and structurally related to this compound. Unfortunately the cell used by GLASSER and GLASSER is not the reduced cell so that its dimensions cannot be compared directly with those of the new form of CaSiO<sub>3</sub>. The transformation from their cell to the reduced cell is

$$\begin{pmatrix} 0 & 0 & 1 \\ 0 & 1 & 0 \\ \bar{1} & 0 & 0 \end{pmatrix}.$$

The reduced-cell dimensions for the two compounds are listed in Table 9. Both compounds have almost identical reduced cells.

In walstromite the silicon atoms also form Si<sub>3</sub>O<sub>9</sub> rings and the Ca atoms are arranged in layers. The Ba atoms connect these Ca layers like the Ca(2) atoms in the high-pressure phase of CaSiO<sub>3</sub>. In both structures the separation of the Ca layers from each other amounts to roughly 5 Å. The orientations of the Ca layers, however,

Table 9. Cell constants of walstromite and high-pressure CaSiO<sub>3</sub>

Cell constants	Walstromite Ca <sub>2</sub> BaSi <sub>3</sub> O <sub>9</sub>		High-pressure CaSiO <sub>3</sub>
	as published	referred to reduced cell	
<i>a</i>	6.733 Å	6.723 Å	6.695 Å
<i>b</i>	9.616 Å	9.616 Å	9.257 Å
<i>c</i>	6.723 Å	6.733 Å	6.666 Å
<i>α</i>	69° 37'	83° 06'	86° 38'
<i>β</i>	102° 20'	77° 40'	76° 08'
<i>γ</i>	96° 54'	69° 37'	70° 23'

are different, as illustrated in Figs. 8*a* and 8*b*. The cell of walstromite contains only two layers which are oriented parallel to (101) and intersect *a* and *c* at  $\frac{1}{2}$ . High-pressure CaSiO<sub>3</sub>, on the other hand, has three layers within its cell which are oriented parallel (111).

As a consequence of the different orientations of the Ca layers in the two structures, an interesting relation in the stacking sequence can be derived. For this purpose both structures will be examined in a direction perpendicular to their layers. A different and larger cell is to be selected so that the Ca layers are parallel to the basal plane

of the new cell. Figures 9 and 10 demonstrate the relation of larger cells labeled  $A$ ,  $B$  and  $C$  with their reduced cell. Figure 9 presents the case of walstromite where the repeat unit along  $C$  contains two layers. Using the large cell as the system of reference, Fig. 11*a* shows that the Ca layers and their adjacent  $\text{Si}_3\text{O}_9$  rings are displaced in respect to each other by the amount  $A/2$ . This shift is indicated in

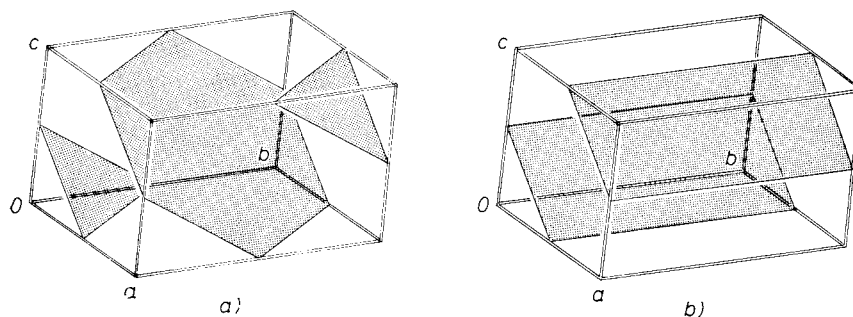


Fig. 8. The orientation of the Ca planes in the reduced cell. The Ca planes are shaded. (a) High-pressure  $\text{CaSiO}_3$ ; (b) Walstromite

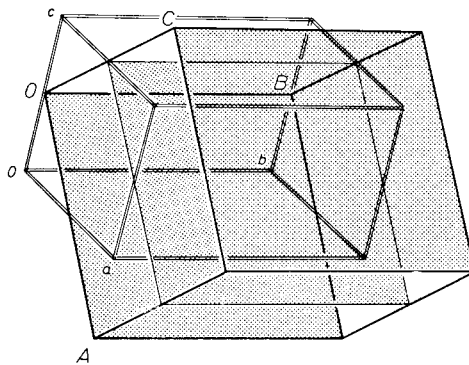


Fig. 9. Walstromite: Selection of a cell whose basal plane is a Ca-O layer. The Ca planes are shaded. The new cell vectors  $A$ ,  $B$ ,  $C$ , expressed in terms of the ones for the reduced cell, are:  $A = a - c$ ,  $B = b$ ,  $C = a + c$

Fig. 11*a* by an arrow on an  $\text{Si}_3\text{O}_9$  ring. On the other hand, in high-pressure  $\text{CaSiO}_3$ , three layers form the repeat unit along  $C$ . In respect to the large cell the layers and their adjacent rings are displaced with respect to each other by the amount  $B/3$ , as indicated by an arrow in Fig. 11*b*. As a consequence the structure of high-pressure  $\text{CaSiO}_3$  can be considered as having layers like the one observed in

walstromite but with each of them shifted by an amount different from the one for walstromite. This structural relation is analogous to a transformation mechanism which requires only chemical bonds reaching to the next layer to be disconnected, the layer itself remains intact. Such a relation corresponds to **BUERGER's** (1961) definition of polytypism in layer structures. Based on this classification, and

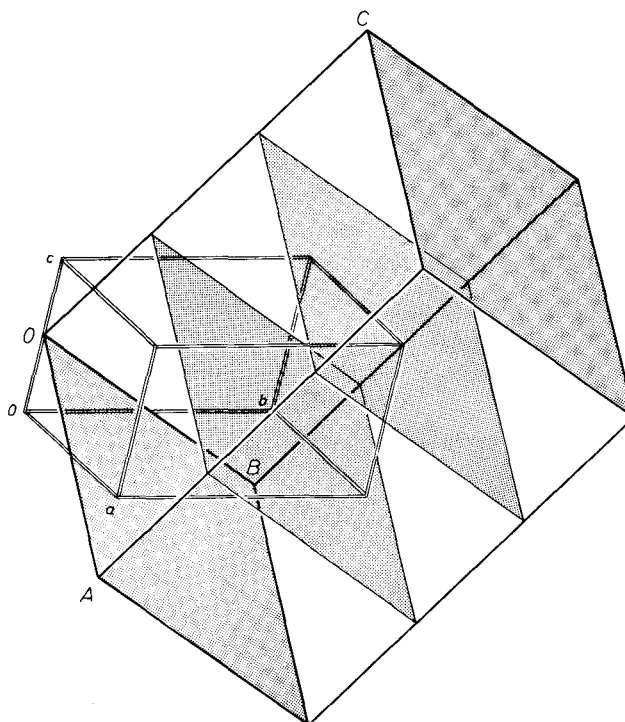


Fig. 10. High-pressure  $\text{CaSiO}_3$ : Selection of a cell whose basal plane is a Ca—O layer. The Ca planes are shaded. The new cell vectors  $A, B, C$ , expressed in terms of the ones for the reduced cell, are:  $A = a - c$ ,  $B = b - c$ ,  $C = b + 2c$

disregarding the substitution of one Ca atom by a Ba atom, it is possible to consider walstromite and this high-pressure phase of  $\text{CaSiO}_3$  to be polytypes.

Since the nature of the structural relation of walstromite and this high-pressure phase of  $\text{CaSiO}_3$  has been established, an additional comparison of both structures with  $\text{SrGeO}_3$  as well as with pseudowollastonite is of great interest. **HILMER** (1963) considered the atomic

arrangement in  $\text{SrGeO}_3$  to be an analog of pseudowollastonite. As mentioned in the discussion of the structure of high-pressure  $\text{CaSiO}_3$ , it is possible to reconstruct complete Ca layers like the Sr layers found in  $\text{SrGeO}_3$  by stuffing the Ca(2) atoms into the voids of the imperfect Ca layers. This reconstruction would require chemical bonds to the nearest neighbors to be broken and would require a change of coordination around Ca(1). Simultaneously, minor displacive adjustments would be necessary. Assuming complete Ca layers, Fig. 11 compares the three structures: walstromite, high-pressure  $\text{CaSiO}_3$ , and pseudowollastonite. In order to stress common structural features, a representation chosen by DORNBERGER-SCHIFF (1962) for  $\text{SrGeO}_3$  is applied to all three compounds. It is evident from Fig. 11 that the Ca atoms

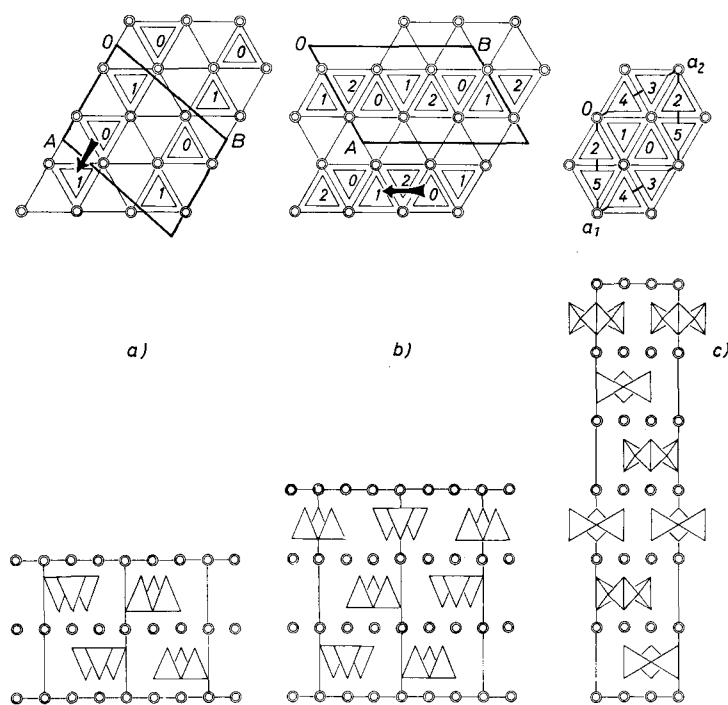


Fig. 11. Stacking sequence of the  $\text{Si}_3\text{O}_9$  rings in walstromite, high-pressure  $\text{CaSiO}_3$ , and pseudowollastonite. For each compound the upper figure represents schematically a projection of the structure onto the Ca layer, while the lower figure is a view parallel to this layer. The double circles are Ca atoms. The numbers give the relative heights of the  $\text{Si}_3\text{O}_9$  rings. (a) Walstromite. The heavy lines outline the cell  $A, B, C$  derived in Fig. 9 (b) High-pressure  $\text{CaSiO}_3$ . The heavy lines outline the cell  $A, B, C$  derived in Fig. 10; (c) Pseudowollastonite, assumed analogous to  $\text{SrGeO}_3$

form a hexagonal network in all three structures. The shapes of the  $\text{Si}_3\text{O}_9$  rings, however, are different. Neglecting small distortions, the rings of walstromite and this compound have symmetry  $3m$  while those of  $\text{SrGeO}_3$ , and possibly pseudowollastonite, have symmetry  $\bar{6}m2$ .

An interesting relation between these structures can be found in the stacking sequence of the rings. HILMER (1963) describes the atomic arrangement of  $\text{SrGeO}_3$ , and hence pseudowollastonite, as follows: The structure is composed of layers having hexagonal symmetry. Six of these layers and their adjacent rings are superposed on one another in such a way that the symmetry for the whole structure is monoclinic. DORNBERGER-SCHIFF (1962) showed that the stacking sequence can be represented graphically by a projection of the structure onto the hexagonal layer as it is shown in Fig. 11c. The relative heights of the rings in a direction perpendicular to the hexagonal layer are labeled with the numbers 0, 1, 2, 3, 4, 5. The lower picture in Fig. 11c shows that the stacking arrangement can be expressed in terms of successive shifts applied on each layer.

Examined in the same manner, this high-pressure phase of  $\text{CaSiO}_3$  shows a repeat unit containing three Ca layers. The  $\text{Si}_3\text{O}_9$  rings, projected onto the hexagonal network, occupy only half of the interstices within a hexagon. The resulting stacking arrangement is similar to that of pseudowollastonite if only half of its repeat unit in a direction perpendicular to the hexagonal network is considered. Walstromite, on the other hand, has only two layers, and the rings associated with them occupy only a third of the interstices within a hexagon.

These structural properties can be summed up in the following way: walstromite, high-pressure  $\text{CaSiO}_3$ , and pseudowollastonite each have hexagonal Ca layers. The three structures can be distinguished by the stacking sequence of the layers and their adjacent rings and by the number of layers in each case. As a consequence it is justifiable to consider pseudowollastonite and high-pressure  $\text{CaSiO}_3$  as polytypes. Since polytypism is a subdivision of polymorphism, one can say that walstromite, the high-pressure phase of  $\text{CaSiO}_3$ , and pseudowollastonite belong to one polymorphic set.

#### Acknowledgement

I wish to thank Professor BUERGER for suggesting the investigation of calcium metasilicates and for his kind advice during the research work. I also thank Dr. CHARLES T. PREWITT for supplying me with

suitable specimens and x-ray powder photographs. I am very grateful to my colleagues Mrs. LYNEVE WALDROP, Dr. PETER SÜSSE, and Dr. HERBERT THURN for valuable discussion and detection of errors. The computations were carried out on an IBM 7094 computer at the Massachusetts Institute of Technology Computation Center. This work was supported by a grant from the National Science Foundation GA-1308.

#### References

- A. W. BARNICK (1936), Strukturuntersuchung des natürlichen Wollastonits. Mitt. K.-Wilh.-Inst. Silikatforsch. No. 172; abstracted in Strukturbericht 4, 207–209.
- M. J. BUERGER (1961), Polymorphism and phase transformations. Fortschr. Min. 39, 9–24.
- M. J. BUERGER and C. T. PREWITT (1961), The crystal structures of wollastonite and pectolite. Proc. Nat. Acad. Sci. 47, 1884–1888.
- K. DORNBERGER-SCHIFF (1962), The symmetry and structure of strontium germanate,  $\text{Sr}(\text{GeO})_3$ , as a structural model for  $\alpha$ -wollastonite,  $\text{Ca}(\text{SiO})_3$ . Soviet Physics—Crystallography 6, 694–700.
- F. P. GLASSER and L. S. DENT GLASSER (1961), Crystallographic study of  $\text{Ca}_2\text{BaSi}_3\text{O}_9$ . Z. Kristallogr. 116, 263–265.
- W. HILMER (1963), An x-ray investigation of strontium germanate  $\text{SrGeO}_3$ . Soviet Physics—Crystallography, 7, 573–576.
- J. W. JEFFERY and L. HELLER (1953), Preliminary x-ray investigation of pseudo-wollastonite. Acta Crystallogr. 6, 807–808.
- J. KARLE and H. HAUPTMAN (1958), Phase determination for colemanite,  $\text{CaB}_3\text{O}_4(\text{OH})_3 \cdot \text{H}_2\text{O}$ . Acta Crystallogr. 11, 757–761.
- F. LIEBAU (1960), Zur Kristallechemie der Silikate, Germanate und Fluoberyllate des Formeltyps  $\text{ABX}_3$ . N. Jahrb. Miner. Abh. 94, 1209–1222.
- KH. S. MAMEDOV and N. V. BELOV (1956), The crystal structure of wollastonite. Doklady Akad. Nauk SSSR 107, 463–466.
- C. T. PREWITT and M. J. BUERGER (1963), Comparison of the crystal structures of wollastonite and pectolite. Min. Soc. Amer. Special Paper 1, 293–302.
- A. E. RINGWOOD and A. MAJOR (1967), Some high-pressure transformations of geophysical significance. Earth and Planetary Science Letters 2, 106–110.
- D. SAYRE (1952), The squaring method: a new method for phase determination. Acta Crystallogr. 5, 60–65.
- F. J. TROJER (1968), The crystal structure of parawollastonite. Z. Kristallogr. 127, 291–308.
- A. DE VRIES (1965), On weights for a least-squares refinement. Acta Crystallogr. 18, 1077–1078.